

Evaporative Cooling and Self-Thermalization in an Open System of Interacting Fermions

Andrey R. Kolovsky* and Dima L. Shepelyansky

Depletion dynamics of an open system of weakly interacting fermions with two-body random interactions is studied. In this model, fermions are escaping from the high-energy one-particle orbitals, that mimics the evaporation process used in laboratory experiments with neutral atoms to cool them to ultra-low temperatures. It is shown that due to self-thermalization the system instantaneously adjusts to the new temperature which decreases with the course of time.

1. Introduction

The cooling of neutral atoms to micro-Kelvin and further to nano-Kelvin temperatures is one of the most noticeable achievements of the modern physics that opened a new era of quantum technologies.^[1] The main method used to cool atoms from micro- to nano-Kelvin temperature is evaporative cooling, where experimental setups are designed to remove the most hot atoms from an atomic cloud. Although being quite successful the method has a drawback that one loses up to 99% of atoms to reach the temperature where Bose or Fermi atoms enter the degenerate state.

To make the method more efficient we need a deeper understanding of the cooling process that can be achieved by considering simplified microscopic models. Up to the best of our knowledge such models were introduced for the first time in refs. [2,3], where it was already noticed that the necessary ingredient of any microscopic model of evaporative cooling is interatomic interactions due to elastic collisions. One needs these collisions to redistribute atoms among the one-particle orbitals (trap modes) when atoms are removed from the high-energy orbitals. This relates the problem of evaporative cooling to the other fundamental problem of physics, namely, self-thermalization in the isolated

system of identical particles. Indeed, it is experimentally known that we can use many concepts of statistical physics for atoms in a trap, in spite of the fact that the system has no contact with a thermostat. Common explanation of the self-thermalization appeals to the theory of Quantum Chaos—a branch of quantum physics dealing with non-integrable systems.^[4,5] Currently there is a growing interest in self-thermalization in various

many-body systems known also as the eigenstate thermalization hypothesis (ETH) and many-body localization (MBL), see recent reviews^[6–9] and the references therein.

In this work we extend our previous studies^[10] of self-thermalization in the closed systems of identical particles onto the open systems, where number of particle is not conserved. Alternatively, the work can be viewed as generalization of the few-mode models^[2,3] of evaporative cooling for arbitrary large number of the modes. As a particular system we consider the so-called two-body random interaction model (TBRIM) which was introduced in the 1970s in nuclear physics in the context of Quantum Chaos.^[11,12] This model describes a system of N spinless fermions distributed over M one-particle orbitals with the energies ϵ_k ($\epsilon_1 \leq \epsilon_2 \leq \dots \leq \epsilon_M$), where fermions have two-body interactions with random matrix elements. We note in passing that the limiting case of this model with strongly interacting fermions recently got a renewed interest in the context of SYK black hole model for theory of quantum gravity.^[13–16] It was shown in refs. [10,17] that at moderate interaction strength TBRIM enters the regime of Quantum Chaos, where its eigenstates $|\Psi_E\rangle$ become self-thermalized. This means, in particular, that occupation numbers $n_k = \langle \Psi_E | \hat{c}_k^\dagger \hat{c}_k | \Psi_E \rangle$ of the one-particle orbitals obeys the Fermi–Dirac distribution

$$n_k = \frac{1}{e^{\beta(\epsilon_k - \mu)} + 1} \quad (1)$$

where the inverse temperature β and the chemical potential μ are uniquely determined by the eigenstate energy E and the number of fermions N in the system. Here we make the system open by introducing particle losses from the most upper orbital. Since we elect to remove particles from the high-energy orbital, the open TBRIM obviously mimics the process of evaporative cooling of fermionic atoms. We argue in the work that the understanding of the self-thermalization mechanism allows to perform an optimization of the evaporative cooling. It involves, in particular, optimization of the rate at which particles are removed from the system. We find that the optimal depletion rate is actually determined by the self-thermalization rate in TBRIM.

Prof. A. R. Kolovsky
Kirensky Institute of Physics
660036 Krasnoyarsk, Russia
E-mail: andrey.r.kolovsky@gmail.com

Prof. A. R. Kolovsky
Siberian Federal University
660041 Krasnoyarsk Russia

Prof. D. L. Shepelyansky
Laboratoire de Physique Théorique
IRSAMC
Université de Toulouse CNRS
UPS
31062 Toulouse, France

 The ORCID identification number(s) for the author(s) of this article can be found under <https://doi.org/10.1002/andp.201900231>

DOI: 10.1002/andp.201900231

2. The Model

The Hamiltonian of the closed (isolated) TBRIM reads

$$\hat{H}^{(N)} = \sum_{k=1}^M \epsilon_k \hat{c}_k^\dagger \hat{c}_k + \epsilon \sum_{ijkl=1}^M J_{ij,kl} \hat{c}_i^\dagger \hat{c}_j^\dagger \hat{c}_k \hat{c}_l \quad (2)$$

where the orbital energies ϵ_k and the interaction (generally complex) constants $J_{ij,kl}$ are random numbers and we set the dispersion of all random entries to unity. The dimension of the Hilbert space is $\mathcal{N}_N = M!/N!(M-N)!$. The parameter ϵ in the Hamiltonian (2) controls the strength of two-body interactions and the super-index N denotes the number of fermions in the system. As mentioned in Section 1, if we increase the interaction strength ϵ the system shows the transition to Quantum Chaos that numerically is observed as a change of the level-spacing statistics from the Poisson distribution to the Wigner–Dyson distribution.^[18] We notice that this transition happens at rather small ϵ_{cr} so that in many aspects fermions can be considered as non-interacting. In particular, the density of states of the system is practically the same as for $\epsilon = 0$. This justifies the usage of the Fermi–Dirac distribution (1) which, strictly speaking, refers to the ideal gas. In what follows we set $\epsilon = 0.008$ and we checked that for this value of ϵ the TBRIM is chaotic and self-thermalized for $2 \leq N \leq 5$, which are relevant for the numerical simulations reported below. It should be stressed that we do not use any average over random entries of the model. In this sense randomness of the orbital energies ϵ_k and interaction constants $J_{ij,kl}$ is not important for physics of the discussed phenomena. However, it simplifies the analysis by insuring, for example, that the mean interaction energy is always around zero and that the system density of states can be approximated by the Gaussian.

We describe the evaporation dynamics by solving the master equation on the system density matrix $\mathcal{R}(t)$

$$\frac{d\mathcal{R}}{dt} = -i[\hat{H}, \mathcal{R}] - \mathcal{L}_{\text{loss}}(\mathcal{R}) \quad (3)$$

$$\mathcal{L}_{\text{loss}}(\mathcal{R}) = \frac{\gamma}{2} (\hat{c}_M^\dagger \hat{c}_M \mathcal{R} - 2\hat{c}_M \mathcal{R} \hat{c}_M^\dagger + \mathcal{R} \hat{c}_M^\dagger \hat{c}_M) \quad (4)$$

where γ is the depletion constant, that is, the rate at which particles are removed from the most upper orbital ϵ_M . Notice that the density matrix \mathcal{R} is defined in the extended Hilbert space given by direct sum of $N_0 + 1$ subspaces where $N_0 = N(t=0)$ is the initial number of fermions. Correspondingly, the Hamiltonian \hat{H} in Equation (3) has block structure with blocks given by Equation (2). In what follows we mainly consider $M = 12$ and $N_0 = 5$ where the total dimension of the Hilbert space is $\mathcal{N} = 1 + 12 + 66 + 220 + 495 + 792 = 3003$. As the initial condition we choose an eigenstate of $\hat{H}^{(N)}$ with $N = N_0$ from the middle of its spectrum. This choice corresponds to infinite effective temperature where occupation numbers of the one-particle orbitals are approximately equal. The quantities which we calculate are the occupation numbers $n_k(t) = \text{Tr}[\hat{c}_k^\dagger \hat{c}_k \mathcal{R}(t)]$, the mean number of fermions in the system, $\bar{N}(t) = \sum_{k=1}^M n_k(t)$, and the mean energy, $\bar{E}(t) = \sum_{k=1}^M \epsilon_k n_k(t)$. Typical behavior of $\bar{N}(t)$ and $\bar{E}(t)$ is exemplified in **Figure 1a,b** where the blue solid and red dashed

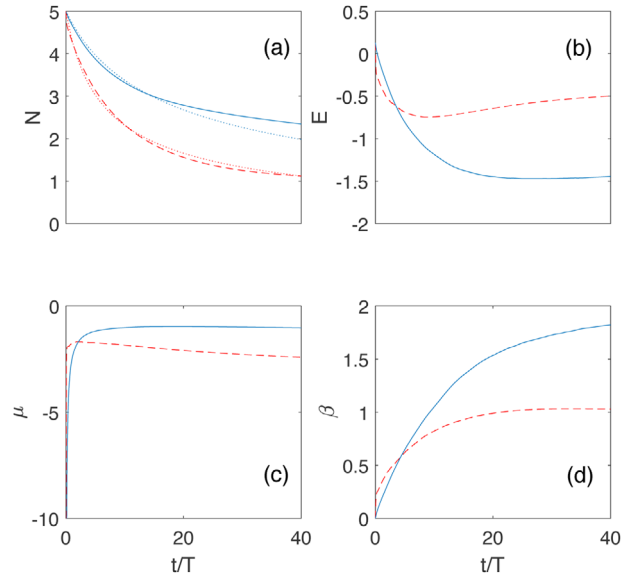


Figure 1. a) The mean number of fermions \bar{N} , b) the mean energy \bar{E} , c) the chemical potential μ , and d) the inverse temperature β as functions of time for the depletion constant $\gamma = 0.2$ (blue solid lines) and $\gamma = 2$ (red dashed lines). Additional dotted lines in panel (a) are Equation (7). The system size is $M = 12$ and initially we have $N_0 = 5$ fermions. Since we set $\hbar = 1$ and $\epsilon_k^2 = 1$, the characteristic time $T = 2\pi$.

lines refer to the case of a small $\gamma = 0.2$ and a large $\gamma = 2$, respectively. In the subsequent two sections we analyze this behavior in some details.

3. Depletion Dynamics

We begin with the depletion dynamics. Similar to the total Hamiltonian, the density matrix $\mathcal{R}(t)$ has block structure where each block $\mathcal{R}^{(N)}(t)$ is associated with the fixed number of fermions in the system. This gives another expression for the mean number of particles

$$\bar{N}(t) = \sum_{N=1}^{N_0} N P_N(t), \quad P_N(t) = \text{Tr}[\mathcal{R}^{(N)}(t)]/N \quad (5)$$

where $P_N(t)$ are interpreted as probabilities to find N particles in the system at a given time t . Probabilities $P_N(t)$ are shown in **Figure 2** in the linear and logarithmic scales for $\gamma = 2$. It is seen that $P_N(t)$ with $N > 1$ show asymptotic exponential decay while $P_1(t)$ approaches unity. This is consistent with the expectation that the steady-state solution of the master equation (3) corresponds to a single fermion. It is also seen in **Figure 2** that relaxation to this steady state is a cascade-like process where “children” cascade takes essentially longer time than “parent” cascade. In the other words, depletion rate decreases proportionally to the number of particles left in the system. In the next paragraph we give a formal explanation for this intuitively expected result and quantify the dependence $\bar{N}(t)$.

One gets a useful insight in the depletion process by analyzing the survival probability, that is, probability to find the initial

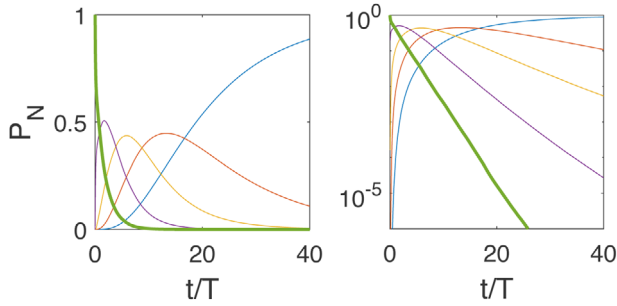


Figure 2. Probabilities $P_N(t)$ to find N particles at a given time t in the linear (left panel) and logarithmic (right panel) scales. Different curves refer (from top to bottom at $t/T = 40$) to $N = 1, 2, 3, 4, 5$, respectively. The survival probability (i.e., the probability to find initial number of fermions) is marked by the thick line. The value of the depletion constant $\gamma = 2$.

number of particles. The survival probability has no parent cascade and can be calculate in a simpler way, namely, by solving the Schrödinger equation with the non-hermitian Hamiltonian \hat{H}_{eff}

$$\hat{H}_{eff}^{(N)} = \sum_{k=1}^M \left(\epsilon_k - i \frac{\gamma}{2} \delta_{k,M} \right) \hat{c}_k^\dagger \hat{c}_k + \epsilon \sum_{ijkl=1}^M J_{ij,kl} \hat{c}_i^\dagger \hat{c}_j^\dagger \hat{c}_k \hat{c}_l \quad (6)$$

which is obtained from the hermitian Hamiltonian (2) by prescribing imaginary energy to the M th orbital. Then the norm of the wave function exactly corresponds to probability to find the initial number of particles in the system. The introduced non-hermitian Hamiltonian (6) relates the currently considered problem to the quantum chaotic scattering.^[19–23] Indeed, considering the Hamiltonian matrix in the Fock basis we find the number of complex diagonal elements to be given by $Q = N \mathcal{N}_N / M$, which can be interpreted as the number of decay channels. It is known that short-time dynamics of the survival probability in chaotic scattering is the exponential decay, $P_N(t) = \exp(-\nu t)$, with increment ν proportional to ratio of the number of channels to the matrix size.^[22,23] Adopting this result to our problem with cascade dynamics (where the number of channels and the matrix size are changing from parent to children cascade) we obtain

$$\bar{N}(t) = N_0 \exp[-\alpha \bar{N}(t) t] \quad (7)$$

where the coefficient α is proportional to the depletion constant γ . The solution of the nonlinear equation (7) is depicted in Figure 1a by dotted lines. It is in reasonable agreement with the straightforward simulation of the depletion dynamics.

At the next step we discuss the dependence of the increment ν for the exponential decay of the survival probability on the depletion constant γ . One may naively expect that ν [and, hence, the coefficient α in Equation (7)] linearly depends on γ . However, this is true only if the depletion constant is smaller than the (yet unspecified) rate of self-thermalization γ_{cr} , while in the opposite case ν actually decreases with an increase of γ . This effect, which is often referred to as the Zeno effect,^[24] has a simple explanation in terms of the energy spectrum of the Hamiltonian (6)

$$\hat{H}_{eff} |\phi_j\rangle = \mathcal{E}_j |\phi_j\rangle, \quad \mathcal{E}_j = E_j - i \frac{\Gamma_j}{2} \quad (8)$$

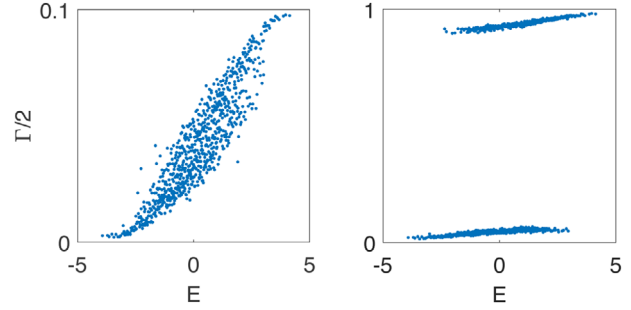


Figure 3. Eigenvalues of the Hamiltonian (6) in the complex plane for $\gamma = 0.2$ (left panel) and $\gamma = 2$ (right panel).

For small γ the complex energies \mathcal{E}_j are located near the real axis, see Figure 3a, and the mean value $\bar{\Gamma}$ of the resonance widths is proportional to γ , $\bar{\Gamma} \sim \gamma$. As γ is increased, the cloud of eigenenergies splits into two groups (in the context of quantum chaotic scattering, this effect is discussed in refs. [20,21]), see Figure 3b. For the first group $\bar{\Gamma}$ remains to be proportional to γ while for the second group we have $\bar{\Gamma} \sim 1/\gamma$, as it is easy to prove by using the first-order perturbation theory. Thus, with an increase of the depletion constant γ the increment $\nu = \bar{\Gamma}$ shows a maximum at some critical value γ_{cr} , which for the parameters of Figure 2 correspond to $\gamma_{cr} \approx 1.2$. We mention that this critical value of the depletion constant can be used as an unambiguous definition of the self-thermalization rate in the considered system of weakly interacting fermions.

4. Thermalization Dynamics

In this section we provide numerically evidence that TBRIM remains to be self-thermalized also in the presence of particle loss. The numerical validation of this statement is given below.

First, using numerical data for the mean number of particle \bar{N} and the mean energy \bar{E} depicted in Figure 1a,b we solve the system of two nonlinear algebraic equation on the chemical potential μ and the inverse temperature β

$$\bar{N} = \sum_{k=1}^M \frac{1}{e^{\beta(\epsilon_k - \mu)} + 1}, \quad \bar{E} = \sum_{k=1}^M \frac{\epsilon_k}{e^{\beta(\epsilon_k - \mu)} + 1} \quad (9)$$

The solution is shown in panels (c) and (d) where, as before, the solid and dashed lines refer to $\gamma = 0.2$ and $\gamma = 2$, respectively. Second, using the obtained μ and β we calculate the occupation numbers according to Equation (1) and compare them with actual occupation numbers calculated as $n_k(t) = \text{Tr}[\hat{c}_k^\dagger \hat{c}_k \mathcal{R}(t)]$, see Figure 4. (From now on we focus on the case $\gamma = 0.2$.) The observed agreement confirms that we indeed have the true thermalization where the notion of temperature is absolutely meaningful, in spite of the absence of any thermal bath. From Figure 1d we clearly see that during evaporation the system temperature decreases with time.

In addition to Figure 4, Figure 5 shows occupation numbers at the beginning and the end of numerical simulation as the function of orbital energies. Remarkably, occupations of two lowest-energy orbitals get increased. Thus, for a larger system size one may expect that n_k of a few lowest-energy orbitals approach unity,

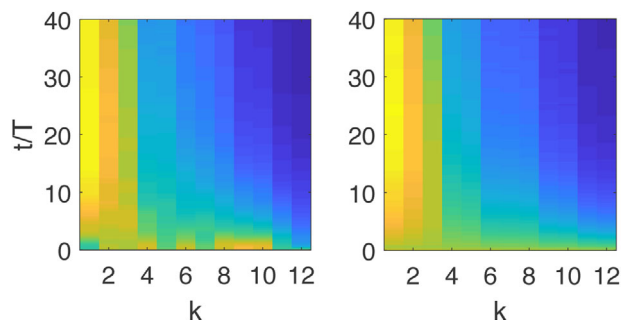


Figure 4. Occupation numbers of the orbitals as a color map (bright yellow=1, dark blue=0), left panel, as compared to the Fermi–Dirac distribution with $\mu = \mu(t)$ and $\beta = \beta(t)$ taken from Figure 1 c,d (right panel).

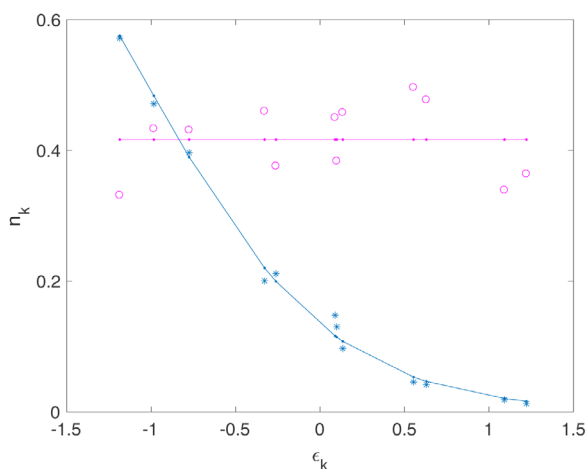


Figure 5. Occupation numbers of the orbitals at the beginning (open circles) and the end (asterisks) of numerical simulation as the function of orbital energies. Solid lines are the Fermi–Dirac distribution for $\beta = 0$ and $\beta \approx 1.8$ that correspond to the initial and final temperature of the system.

that is, we enter the degenerate state. This expectation is supported by results of numerical simulation for $M = 16$ and $N_0 = 8$ (the total dimension of the Hilbert space $\mathcal{N} = 39\,203$), where occupation numbers of the four lowest orbitals are above 0.5 and occupations of the two lowest orbitals are above 0.7.

5. Case of SYK Black Hole Model

Due to a significant recent interest in the SYK model,^[13–16] we briefly discuss the evaporation process in this model which corresponds to vanishing orbital energies $\epsilon_k = 0$ in the Hamiltonian (2). Clearly, in this case of strongly interacting fermions we cannot appeal to the Fermi–Dirac distribution (which is derived for non-interacting fermions). However, we still can address the depletion dynamics.

As for the previous TBRIM case, we assume fermions to escape only from one orbital. Upper panels in **Figure 6** shows probabilities $P_N(t)$ for $\gamma = 2$ in the linear and logarithmic scales. The decay rate of the survival probability is seen to be slightly larger than in the TBRIM case, which is consistent with distribution of eigenvalues of the non-Hermitian Hamiltonian—see lower panels in **Figure 6** where we depict the eigenvalue distribution for

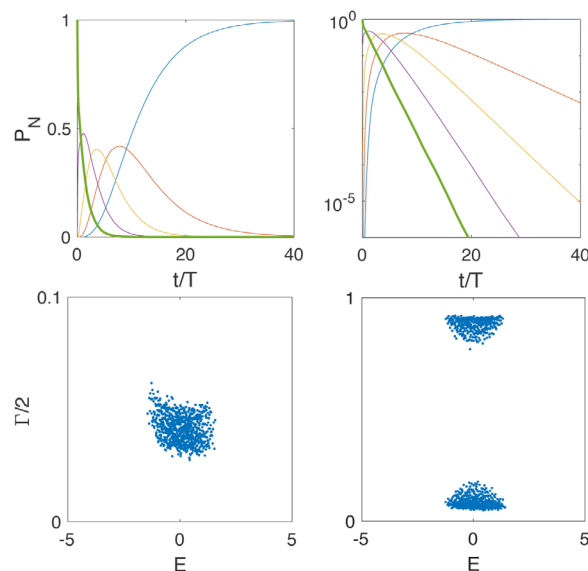


Figure 6. Top panels: the same as in **Figure 2** yet for the SYK case where one-particle energies ϵ_k in the Hamiltonian (2) are set to zero. Bottom panels: the same as **Figure 3** yet for the SYK case where ϵ_k in the Hamiltonian (6) are set to zero.

$\gamma = 0.2$ and $\gamma = 2$. Similar to the TBRIM case, the compact cloud of eigenvalues is found to separate into two clouds at $\gamma \approx 1.2$. Thus for both TBRIM and SYK models the depletion rate is maximized at the same value of γ_{cr} .

6. Conclusions

We analyzed the process of evaporative cooling in the system of weakly interacting fermions. This process has a competition between depletion, where particles are removed from high-energy one-particle orbitals (generalization of the results onto the case of more than one decaying orbital is straightforward) and self-thermalization, which repopulates these orbitals. We especially stress the importance of the latter process. It is generally a hard problem to find conditions for emergence of self-thermalization in a given system of interacting particles. For the isolated TBRM these conditions have been analyzed in our previous works.^[10,17] In the present work we showed that the self-thermalization in TBRIM takes place also in the presence of particle loss (decay). Thus the TBRIM becomes a paradigmatic model for investigation of different aspects of self-thermalization in closed and open systems.

We studied the depletion dynamics in the open TBRM by mapping the problem to quantum chaotic scattering. It was shown, in particular, that the number of lost particles is not a monotonic function of the depletion constant γ but has a pronounced maximum at some γ_{cr} . Since the depletion constant can be varied in laboratory experiments, this result suggests a method for measuring the self-thermalization rate by finding the critical γ_{cr} , where the increment ν for exponential decay of the survival probability is maximized.

Since we remove particles from the high-energy orbitals, the depletion process results in a decrease of the system energy and,

as a consequence, in the temperature drop for the remaining particles. We stress that efficiency of this cooling mechanism is not just proportional to particle loss, as one might naively expect, but is an involved function of the depletion constant γ (which can be varied in a laboratory experiment), the self-thermalization rate γ_{cr} (which is an internal property of the system), and the duration of the evaporation process (which can be limited by some reason). An example is given in Figure 1a,d. It is seen that within the same time interval we reached lower temperature for $\gamma = 0.2$ than for $\gamma = 2$, in spite of the fact that in the former case we lost less particles than in the latter case.

Acknowledgements

For D.L.S. this work was supported in part by the Programme Investissements d'Avenir ANR-11-IDEX-0002-02, reference ANR-10-LABX-0037-NEXT (project THETRACOM). For A.R.K. this work was supported in part by Russian Science Foundation through the grant N19-12-00167.

Conflict of Interest

The authors declare no conflict of interest.

Keywords

open quantum systems, quantum chaos, self-thermalization

Received: May 28, 2019

Revised: September 5, 2019

Published online:

- [1] J. P. Dowling, G. J. Milburn, *Phil. Trans. R. Soc. A* **2003**, 361, 3655.
- [2] R. Quadt, H. Wiseman, D. Walls, *Phys. Lett. A* **1996**, 219, 19.
- [3] M. Holland, K. Burnett, C. Gardiner, J. I. Cirac, P. Zoller, *Phys. Rev. A* **1996**, 54, 1757(R).
- [4] F. Haake, *Quantum Signatures of Chaos*, Springer, Berlin **2010**.
- [5] H.-J. Stöckmann, *Quantum Chaos: An Introduction*, Cambridge University Press, Cambridge **2000**.
- [6] R. Nandkishore, D. A. Huse, *Annu. Rev. Condens. Matter Phys.* **2015**, 6, 15.
- [7] L. D'Alessio, Y. Kafri, A. Polkovnikov, M. Rigol, *Adv. Phys.* **2016**, 65, 239.
- [8] F. Borgonovi, F. M. Izrailev, L. F. Santos, V. G. Zelevinsky, *Phys. Rep.* **2016**, 626, 1.
- [9] F. Alet, N. Laflorencie, *C. R. Phys.* **2018**, 19, 498.
- [10] A. R. Kolovsky, D. L. Shepelyansky, *Erophys. Lett.* **2017**, 117, 10003.
- [11] O. Bohigas, J. Flores, *Phys. Lett. B* **1971**, 35, 383.
- [12] J. French, S. Wong, *Phys. Lett. B* **1971**, 35, 5.
- [13] A. Kitaev, *A Simple Model of Quantum Holography*, Video talks at KITP Santa Barbara, **2015**.
- [14] S. Sachdev, *Phys. Rev. X* **2015**, 5, 041025.
- [15] J. Polchinski, V. Rosenhaus, *J. High Energ. Phys.* **2016**, 2016, 1.
- [16] J. Maldacena, D. Stanford, *Phys. Rev. D* **2016**, 94, 106002.
- [17] K. M. Frahm, D. L. Shepelyansky, *Eur. Phys. J. B* **2018**, 91, 257.
- [18] P. Jacquod, D. L. Shepelyansky, *Phys. Rev. Lett.* **1997**, 79, 1837.
- [19] V. V. Sokolov, V. G. Zelevinsky, *Phys. Lett. B* **1988**, 202, 10.
- [20] F. Haake, F. Izrailev, N. Lehmann, D. Saher, H.-J. Sommers, *Z. Phys. B* **1992**, 88, 359.
- [21] N. Lehmann, D. Saher, V. V. Sokolov, H.-J. Sommers, *Nucl. Phys. A* **1995**, 582, 223.
- [22] D. V. Savin, V. V. Sokolov, *Phys. Rev. E* **1997**, 56, R4911.
- [23] M. Glück, A. R. Kolovsky, H.-J. Korsch, *Physica E* **2001**, 9, 478.
- [24] B. Misra, E. C. G. Sudarshan, *J. Math. Phys.* **1997**, 18, 756.